Bioaccumulation of inorganic and organic mercury in the cuttlefish Sepia officinalis: influence of ocean acidification and food type

Antoine Minet, Marc Metian, Angus Taylor, Sophie Gentès, Sabine Azemard, François Oberhänsli, Peter Swarzenski, Paco Bustamante, Thomas Lacoue-Labarthe

Bioaccumulation of inorganic and organic mercury in the cuttlefish *Sepia officinalis:* influence of ocean acidification and food type

Antoine MINET[1], Marc METIAN[2], Angus TAYLOR[2], Sophie GENTÈS[1], Sabine AZEMARD[2], François OBERHÄNSLI[2], Peter SWARZENSKI[2], Paco BUSTAMANTE[1,3], Thomas LACOUE-LABARTHE[1]

[1] *Littoral Environnement et Sociétés (LIENSs), UMR 7266 CNRS - La Rochelle Université, 2 rue Olympe de Gouges, 17000 La Rochelle, France*

[2] *International Atomic Energy Agency (IAEA), Environment Laboratories, 4 Quai Antoine Ier, 98000 Principality of Monaco*

[3] *Institut Universitaire de France (IUF), 1 rue Descartes 75005 Paris, France*

Corresponding author: Antoine Minet (email: minet.antoine.etu@gmail.com / tel: +33 5 16 49 67 23)

Highlights

- Waterborne $i^{203}Hg$ is efficiently taken up but lost with a biological $T_{1/2}$ of ~50d
- Dietary $Me^{203}Hg$ is highly assimilated (>95%) and indefinitely retained
- Proportion of MeHg in prey defines the Hg kinetics in cuttlefish
- pH had no effect on bioaccumulation and tissue distribution of Hg in cuttlefish
- Trophic pathway is the main route of Hg bioaccumulation in cuttlefish

Graphical abstract

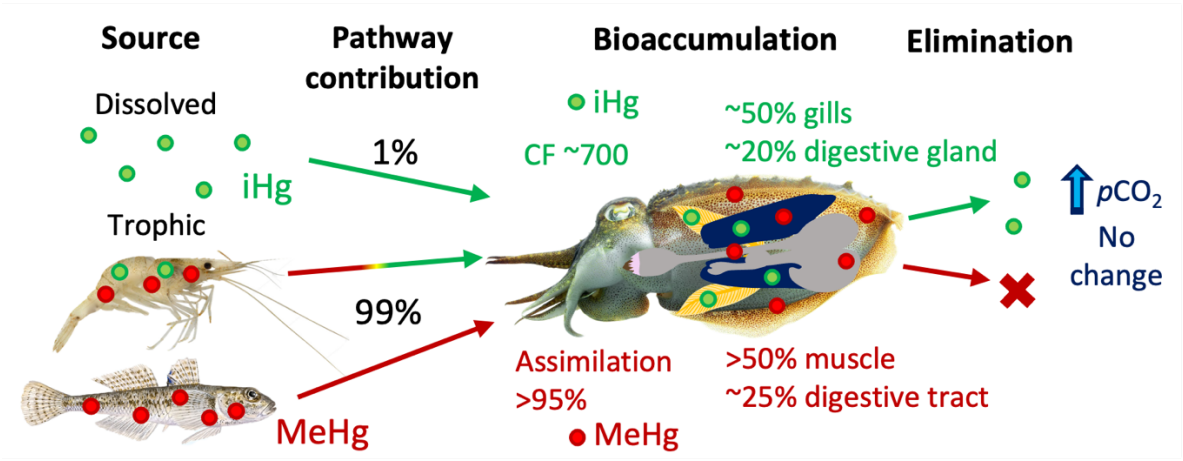

Abstract

The bioaccumulation of mercury (Hg) in marine organisms through various pathways has not yet been fully explored, particularly in cephalopods. This study utilises radiotracer techniques using the isotope ^{203}Hg to investigate the toxicokinetics and the organotropism of waterborne inorganic Hg (iHg) and dietary inorganic and organic Hg (methylHg, MeHg) in juvenile common cuttlefish *Sepia officinalis*. The effect of two contrasting CO_2 partial pressures in seawater (400 and 1600 µatm, equivalent to pH 8.08 and 7.54 respectively) and two types of prey (fish and shrimp) were tested as potential driving factors of Hg bioaccumulation. After 14 days of waterborne exposure, juvenile cuttlefish showed a stable concentration factor of 709±54 and 893±117 at pH 8.08 and 7.54, respectively. The accumulated dissolved i^{203}Hg was depurated relatively rapidly with a radiotracer biological half-life ($Tb_{1/2}$) of 44±12 and 55±16 days at pH 8.08 and 7.54, respectively. During the whole exposure period, approximately half of the i^{203}Hg was found in the gills, but i^{203}Hg also increased in the digestive gland. When fed with ^{203}Hg-radiolabelled prey, cuttlefish assimilated almost all the Hg provided (>95%) independently of the prey type. Nevertheless, the prey type played a major role on the depuration kinetics with Hg $Tb_{1/2}$ approaching infinity in fish fed cuttlefish *vs.* 25 days in shrimp fed cuttlefish. Such a difference is explained by the different proportion of Hg species in the prey, with fish prey containing more than 80% of MeHg *vs.* only 30% in shrimp. Four days after ingestion of radiolabelled food, iHg was primarily found in the digestive organs while MeHg was transferred towards the muscular tissues. No significant effect of pH/pCO_2 variation was observed during both the waterborne and dietary exposures on the bioaccumulation kinetics and tissue distribution of i^{203}Hg and Me^{203}Hg. Dietary exposure is the predominant pathway of Hg bioaccumulation in juvenile cuttlefish.

Keywords: cephalopod; radiotracer; methylmercury, iHg; waterborne contamination, trophic transfer; kinetics; organotropism.

Introduction

As a trace element, mercury (Hg) mostly derives both from natural sources such as volcanic eruptions or weathering and from anthropogenic sources (*e.g*. mining, coals use). Through atmospheric deposition, ocean uptake or river release (Sonke *et al.*, 2018; Jiskra *et al.*, 2021), Hg is found as (1) inorganic (iHg) free forms and complex ions which is its primary form in seawater, and (2) organic forms, most commonly as methylmercury (MeHg), resulting from iHg methylation by microorganisms (Benoit *et al.*, 2002). MeHg is well known for its efficient bioaccumulation in biota, biomagnification along food webs and its high toxicity, especially its neurotoxicity (Bisi *et al.*, 2012; van der Velden *et al.*, 2013; Chouvelon *et al.*, 2018). In the marine environment, organisms are simultaneously exposed to both forms of Hg from both dissolved and dietary pathways. This cumulative exposure dictates the level of bioaccumulated total Hg, its body distribution, and by consequence its potential toxic effects. Among marine organisms, most of the available information on Hg is related to top predators (fish, mammals, and birds) and seafood, due to their high Hg concentrations and their associated risks as an important food source for humans. In contrast, information on Hg in cephalopods is still scarce, despite the fact that these molluscs: 1) are known to efficiently accumulate Hg reaching up to more than 3 µg g^{-1} dry weight (dw) in muscle (*e.g*., Barghigiani et al., 2000); 2) have a pivotal place in trophic webs playing a key role in the transfer of Hg to top predators (Jackson *et al.*, 2006; Carravieri *et al.*, 2014) and 3) have a developed central nervous system potentially affected by Hg accumulation (Minet et al., 2021).

Among cephalopods, the cuttlefish *Sepia officinalis* is one of the most abundant and harvested species from the northern east Atlantic. In the English Channel and the Bay of Biscay, the one or two-year old mature cuttlefish colonise the coastal waters in spring to mate and to spawn before dying (Boucaud-Camou and Boismery, 1991). After ~ 2 months of embryonic development, the juveniles grow on the coastal nurseries where they found appropriate food in both quantity and quality (Pinczon du Sel *et al.*, 2000). Although known as opportunistic predators, juveniles fed mainly on small crustaceans (amphipods and/or shrimps) during the first 3 months after which fish constitute the main prey

(Pinczon du Sel *et al.*, 2000). Thus, as the nature of prey could play a key role in the efficiency of metal assimilation by predators (Pouil *et al.*, 2016), it was advisable to reconsider Hg bioaccumulation taking into account various relevant prey.

Concomitantly, the ocean is becoming more acidic (Gattuso and Hansson, 2011) because the atmospheric carbon dioxide (CO_2) emissions have been steadily increasing for decades due to anthropogenic activities. The recent IPPC models predicted that the partial pressure of CO_2 (pCO_2) will raise until 500 and 1200 µatm according to the SSPI 4.5 and SSPI 8.5 scenario by the end of century (IPCC 2021). Consequently, atmospheric CO_2 dissolves in seawater leading to an increase of pCO_2 in the ocean surface, resulting in a reduction of seawater pH of 0.4 pH unit (IPCC 2021). This specific change of seawater chemistry, known as Ocean Acidification (OA), is directly affecting the carbonate-silicate cycle, and therefore also impacting calcifying organisms (Kroeker *et al.*, 2010). Moreover, such seawater changes may also induce physiological and behavioural alterations in marine organisms (Pörtner and Farrell, 2008; Stumpp *et al.*, 2011; Nilsson *et al.*, 2012; Dorey *et al.*, 2013; Ramaglia *et al.*, 2018) and is a real threat to ecosystems.

The chemical speciation that drives the bioavailability of trace elements in seawater and their subsequent bioaccumulation by marine organisms is also closely related to the seawater pH (Shi *et al.*, 2016; Stockdale *et al.*, 2016; Belivermiş *et al.*, 2020). The OA leads to a decrease of OH^- and CO_3^{2-} ions concentrations and can affect the solubility, adsorption, toxicity, and rates of redox processes of metals in seawater (Millero *et al.*, 2009). However, metals that form strong complexes with chloride (*e.g*. Hg) will see little if any change in speciation because chloride concentration will not change (Millero *et al.*, 2009). Nevertheless, the increase of seawater H^+ could lead to cation competition for biological bindings site and affect the bioaccumulation of trace elements (*e.g*. Pascal *et al.*, 2010). As previously indicated, the acidified conditions can affect marine organisms, especially specific metabolic processes connected to element bioaccumulation such as the ion regulatory systems, and so will affect the acid-base balance, ion exchange, respiration rate and digestion efficiency of multiple invertebrate species (Melzner *et al.*, 2020). In the case of Hg, it has been hypothesized that pH has a direct effect

on its speciation, bioavailability bioconcentration, trophic transfer and depuration (Gworek *et al.*, 2016). For instance, a moderately elevated level of pCO_2 (*i.e*. 850 µatm, equivalent to a pH of 7.85) increased the accumulation of dissolved iHg in the paralarvae of squid *Loligo vulgaris* (Lacoue-Labarthe *et al.*, 2011), while multigenerational exposure to dissolved iHg and high pCO_2 (*i.e*. 1000 µatm, pH 7.70) resulted in a lower accumulation and toxicity of Hg on the copepod *Tigriopus japonicus* (Li *et al.*, 2017). In the same way, elevated pCO_2 (1100 µatm, pH 7.50) decreased dietary MeHg accumulation and consistently lead to a dampening effect on warming- and contamination-elicited oxidative stress and heat shock responses in the meagre *Argyrosomus regius* (Sampaio *et al.*, 2018).

In this context, the present work aims at determining the processes of total Hg bioaccumulation in the coastal juvenile cuttlefish, considering that they are mainly exposed 1) to dissolved iHg in seawater and 2) to MeHg, and iHg to a lesser extent, contained in their prey, whose respective concentrations and bioavailability could vary among prey types. The bioaccumulation processes were assessed through a toxicokinetic approach using radioisotope as tracer of Hg, allowing accurate and individualised measurements at the whole body level during exposure and depuration phases (Warnau and Bustamante, 2007). Kinetics parameters, *i.e*. the uptake (ku) and depuration (ke) rates, and the assimilation efficiencies (AE), were used to calculate the contribution of both bioaccumulation pathways and were also discussed with respect to the prey type (*i.e.* shrimp vs fish) and the seawater pCO_2 levels as environmental factors modulating the Hg bioaccumulation efficiencies and organotropism in cuttlefish juvenile.

Material and methods

Cuttlefish collection

One-month old juveniles of the common cuttlefish *Sepia officinalis* were caught by dip net in the intertidal eelgrass beds from Arcachon Bay, France (Atlantic coast of southwestern France: 44°41'14.0"N; 1°14'00.6"W) in summer 2019 (n = 60; mantle length = 47 ± 13 mm). Individuals were acclimated for 3 weeks in open-circuit glass aquariums (flux: 60 L h^{-1}; salinity: 38; temperature: 19 ± 0.2°C; pH: 8.08 ± 0.03; 12h light:12h dark cycle) at the International Atomic Energy Agency, Marine Environment Laboratories (IAEA-EL) premises in Monaco. Cuttlefish were fed with live ditch shrimp *Palaemon varians* or live green shore crabs *Carcinus maenas* twice a day known as being preferential prey for juveniles (Blanc *et al.*, 1998; Darmaillacq *et al.*, 2004). The experiments were the subject of an authorization request for the use of animals for scientific purposes, referenced and authorized under the number APAFIS # 20520-2019050614554709.

Radiotracer

A radiotracer solution of $i^{203}Hg$ (2107.4 kBq L^{-1}) was prepared in 1 N nitric acid from a carrier-free parent stock solution (as $^{203}HgCl_2$; $T_{1/2}$ = 46.59 days) provided by Eckert & Ziegler. Then, a solution of radiolabelled $Me^{203}Hg$ was obtained by methylation of $i^{203}Hg$ according to Rouleau and Block (1997). Briefly, (1) A portion of 1 mL or less of a radioactive $^{203}HgCl_2$ solution (in 0.1–0.01 M HCl) was placed in a 100-mL separatory funnel fitted with a Teflon® stopcock. The contents of a 25-mg vial (18.6 mmol) of MeCo (Sigma), dissolved in 0.01 M HCl just before use so that the total volume was 2 mL, were added. The funnel was wrapped in aluminium foil to protect it from light and left to stand for 1 h. (2) 10 mL of hexane/benzene (1:1) were added and the mixture was stirred for 10 min, by using a mechanical stirrer equipped with a glass stirring rod, the bottom of which was flattened and twisted so that the stirred solutions would be directed down-wards. The extraction was repeated twice, and the organic layers were combined in a 50-mL conical glass tube containing 2 mL of a 0.005 M Na_2CO_3 solution. (3) The combined organic layers were stirred over the Na_2CO_3 solution for 10 min, then

evaporated by blowing a gentle stream of clean air or nitrogen over the surface. The radioactive $CH_3{}^{203}Hg(II)$ (*i.e*. $Me^{203}Hg$) was left dissolved in the Na_2CO_3 solution. The $Me^{203}Hg$ solution was gamma-counted to determine the final yield of methylation (95%).

Dissolved $i^{203}Hg$ exposure

Twenty-four cuttlefish were evenly divided into six 70 L aquaria (3 replicates x 2 pH levels; close-water system 0.45 µm filtered natural seawater, T = 19°C; Salinity = 38; constantly aerated; NO_2^- < 0.1 mg L^{-1}, NO_3^- < 5mg L^{-1}) and left two weeks for acclimatisation to the experimental rearing conditions. During this period, each individual was gently handled daily and placed in 200 mL plastic containers in order to accustom them to sampling and gamma-counting conditions (see section below) and thus limit their stress during the experiment. From the beginning of this period, three aquaria were maintained at the ambient seawater pH/pCO_2 (*i.e*. control: pH = 8.08 ± 0.06 equivalent to 400 µatm) while the pH/pCO_2 in the three other aquaria were progressively lowered during 4 days until a value of ~ 7.6 (*i.e*. acidified condition: pH = 7.54 ± 0.04 equivalent to 1600 µatm), consistently with modelled scenarios of ocean pH at the end of the century (*i.e*. SSPI 8.5, IPPC, 2021). Briefly, the pCO_2 was regulated by an IKS system from Aquastar© with pH measurements every 20 min and a weekly calibration of the IKS probes with NBS standard pH solution (pH 4.0 and pH 7.0), a glass electrode (Metrohm©, ecotrode plus) and using TRIS buffer solutions (salinity 35, provided by A. Dickson, Scripps university, USA). Total alkalinity was measured potentiometrically using a Metrohm© titrator (Titrando 888). The pH values expressed in the NBS scale were corrected and expressed on the total scale using values of total alkalinity and carbonate chemistry parameters calculated with seacarb package from R (Gattuso *et al.*, 2021). Experimental conditions are outlined in Table S1.

Following acclimatisation, cuttlefish were exposed for 14 days to dissolved $i^{203}Hg$ by spiking 10 µL of the radiotracer solution in order to reach 0.2 kBq L^{-1} of ^{203}Hg in each aquarium. This activity corresponded to an addition of less than 5 ng L^{-1} of Hg. The seawater was spiked every day the first week and every second day the second week, after each water renewal. Radiotracer activities in

seawater from each aquarium were checked before and after each water renewal by gamma counting (see below) showing a mean exposure throughout the uptake phase of 215 ± 76 Bq L^{-1} of $i^{203}Hg$. During this uptake phase, the cuttlefish were fed daily with 2 live ditch shrimps between water renewal and new spikes to avoid contamination through dietary pathway. At different time intervals (*i.e*. at days 1, 2, 3, 4, 7, 9, 11 and 14), all individually identified cuttlefish were whole body gamma-counted alive. Each individual was held isolated in separate circular plastic containers and counted with Germanium detectors (counting description below).

Following this uptake phase, the water was renewed with natural seawater and the aquaria were kept in open-circuit (flux: 60 L h^{-1}) for 21 days to follow the loss of ^{203}Hg in contaminated juveniles. During this depuration phase, individuals were gamma-counted on days 1, 2, 3, 4, 7, 9, 11, 14, 17 and 21. In addition, 1 individual per aquarium was sampled (n=3 per condition) and dissected to investigate the radiotracer distribution among the beak (BE), the branchial hearts (BH), the digestive gland (DG), the digestive tract (DT), the gills (G), the mantle muscles (M), the optic lobes (OL), the tentacles and arms (TA) and the remaining tissues (R) at day 7 and 14 of the exposure phase and the remaining 2 individuals per aquaria (n = 6 per condition) at day 21 of the depuration phase (see schematic summary Fig. S1).

Trophic $Me^{203}Hg$ exposure

The ^{203}Hg bioaccumulation by trophic route was assessed using the pulse-chase feeding method (Metian *et al.*, 2008) considering two types of prey (*i.e*. shrimp and fish). Both the ditch shrimp *Palaemon varians* and the sand goby *Pomatoschistus microps* were collected in Atlantic saltmarshes near La Rochelle, France. In addition, the effect of lowering pH/elevated pCO_2 on the Hg trophic transfer was tested for fish as prey. Thus, the chosen preys were radiolabelled according to a two-step procedure: first, commercial fish pellets and frozen brine shrimp were carefully spread in two glass petri dishes, spiked with $Me^{203}Hg$ in seawater and were left to evaporate overnight under a fume hood, in order to achieve an activity of ~ 100 Bq g^{-1}. Sand gobies and common ditch shrimps were then fed

ad libitum during 3 days with this Me^{203}Hg radiolabelled food (*i.e*. fish pellets and brine shrimps, respectively) in open-circuit aquaria, until reaching a whole-body total ^{203}Hg activity of at least 100 Bq per prey. In addition, four individuals of both species were sampled and analysed to investigate the ^{203}Hg speciation, *i.e*. the i^{203}Hg and ^{203}MeHg proportions for both prey type using the protocol described by Azemard and Vassileva (2015).

Thirty-six cuttlefish were evenly divided into 9 open-circuit 30 L aquaria (T = 19°C; Salinity = 38, flux: 60 L.h^{-1}) corresponding to 3 replicates x 3 experimental conditions; cuttlefish were fed with: 1) ^{203}Hg radiolabelled ditch shrimp at ambient pH (*i.e*. pH = 8.08), with 2) ^{203}Hg radiolabelled sand goby at ambient pH and 3) ^{203}Hg radiolabelled sand goby at lowered pH (*e.g*. pH = 7.54).

Following a 2-week acclimatisation period as previously described, the cuttlefish were starved for 1 day before being fed with a single ^{203}Hg radiolabelled prey. All individuals were then whole-body gamma-counted alive just after the radiolabelled feeding, and then at the different time intervals (*i.e*. at days 1, 2, 3, 4, 6, 8, 10, 14, 17 and 21) over a 21-d period to follow the depuration kinetic of ^{203}Hg along the experimental course. Finally, at days 4 and 21, one individual per aquaria (n = 3 per condition) and three individuals per aquaria (n = 9 per condition), respectively, were sampled, weighed, and dissected to determine the radiotracer distribution among the same organs as previously listed for the dissolved i^{203}Hg exposure. The dissection on day 4 allowed for a visualisation in the short term as to how the ^{203}Hg is taken care of after ingestion, while day 21 allowed for a longer-term study of ^{203}Hg translocation and/or depuration (see schematic summary Fig. S2).

Radioanalyses and data treatment

The ^{203}Hg radioactivity in each sample was measured using a high-resolution γ-spectrometry system consisting of 4 coaxial High Purity Germanium (HPGe; N- or P- type) detectors (EGNC 33-195-R, Canberra® and Eurysis®) connected to a multi-channel analyser and a computer equipped with spectra analysis software (Interwinner® 6 and 8). The detectors were calibrated with an appropriate standard for each counting geometry used and measurements were corrected for background and physical

decay of the radiotracer. Juvenile cuttlefish and dissected tissues were placed in circular plastics boxes (10 cm diameter, 5 cm height) and glass tubes (1 cm diameter, 5 cm height) respectively and measured with the detectors. The counting times for the juveniles alive ranged from 10 to 30 min to obtain counting errors less than 5% and maintain a good animal welfare and normal behaviour. Samples of tissues and organs were counted from 10 min to 24 h, depending on the total ^{203}Hg activity, until obtaining counting errors less than 5%.

The uptake of dissolved i^{203}Hg from seawater was expressed as change in concentration factors (CF; ratio between radiotracer content in the juvenile, Bq g^{-1}ww, and time-integrated activity in seawater, Bq g^{-1}) over time (Warnau *et al.*, 1996). The uptake kinetic was then described by a saturation exponential model:

$$CF_t = CF_{ss}(1 - e^{-k_e t})$$

where CF_t and CF_{ss} are the concentration factors at time t (d) and at steady state (ss), respectively, and k_e is the biological depuration rate constant (d^{-1}) (Whicker and Schultz, 1982).

The radiotracer depuration kinetics were expressed in terms of the change in percentage of the remaining activity (*i.e*. radioactivity at time t divided by initial radioactivity measured in the organisms or in the tissue at the beginning of the depuration period × 100) over time. The depuration kinetics was fitted according to the single exponential equation:

$$A_t = A_0 e^{-k_e t}$$

where A_t and A_0 are the remaining activities (%) at times t (d) and 0, respectively. The determination of k_e allows the calculation of ^{203}Hg biological half-life ($Tb_{1/2} = \ln 2/k_e$). In the context of the seawater and feeding experiments, A_0 represents the absorption ($A_{0,w}$) and the assimilation efficiencies (AE), respectively.

Bioaccumulation model

The relative contribution of each uptake pathway was determined using the bioaccumulation model originally proposed by Thomann (1981) and revised by Thomann *et al.* (1995) and Metian *et al.* (2008). In this model, the total concentration of Hg in the juveniles, C_t (ng g^{-1}) is equal to the sum of each concentration resulting from the incorporation of Hg via the different pathways:

$$C_t = C_{f,ss} + C_{w,ss}$$

where $C_{f,ss}$ is the food-derived Hg concentration (ng.g^{-1}) in juveniles at steady state :

$$C_{f,ss} = \frac{AE \times IR \times C_f}{k_{e,f}}$$

and $C_{w,ss}$ the water-derived Hg concentration (ng g^{-1}) in juveniles at steady state :

$$C_{w,ss} = \frac{A_{0,w} \times k_{u,w} \times C_w}{k_{e,w}}$$

where $A_{0,w}$ is the absorption efficiency (%) of the Hg from seawater, AE is the assimilation efficiency (%) of the Hg from food, C_f and C_w are the Hg activities in food and seawater (ng g^{-1} and ng mL^{-1}, respectively), respectively, IR is the ingestion rate (g g^{-1} d^{-1}), $k_{u,w}$ is the uptake rate constant (d^{-1}) from seawater and $k_{e,f}$ and $k_{e,w}$ are the biological depuration rate constants (d^{-1}) for food and water pathways, respectively. The relative contribution (%) of each contamination pathway is then assessed from the following relationships:

$$\%\, food = \frac{C_{f,ss}}{C_{f,ss} + C_{w,ss}} \times 100$$

$$\%\, seawater = \frac{C_{w,ss}}{C_{f,ss} + C_{w,ss}} \times 100$$

Constants (and their statistics) of the fitting equations were estimated by iterative adjustment of the models using the nls curve-fitting routine in R version 3.6.1 (R Core Team, 2019). Then, the uptake and loss kinetics parameters (*i.e.* CF_{ss}, k_u, $A_{0,w}$, AE, $k_{e,w}$, $k_{e,f}$) were determined for each individual, considering that the best fitting model obtained for the entire set of cuttlefish was applied to individuals. The comparisons of CF_{ss}, k_u and k_e values following waterborne exposure, between both pH conditions were performed using one-way ANOVA. The comparison of AE and $k_{e,f}$ among treatments, following

dietary experiment, were tested using a two-way ANOVA with pH and prey as categorial factors. The level of significance for statistical analysis was set at $\alpha = 0.05$.

Results

Exposure to dissolved $i^{203}Hg$

The uptake kinetics of dissolved $i^{203}Hg$ in whole-body cuttlefish were best fitted by a saturation exponential model, regardless of pH, with a calculated CF_{ss} of 709 ± 54 and 894 ± 117 at pH 8.08 and 7.54, respectively (mean ± SD; Fig. 1A, Table 1). After the 14-day exposure period, non-contaminating conditions were restored and the depuration kinetics of $i^{203}Hg$ were followed for 21 days for both pH conditions. The $i^{203}Hg$ depuration kinetics were best described by a mono-exponential model (Fig. 1B, Table 1) regardless of pH, indicating that the whole $i^{203}Hg$ (*i.e*. 96 **±** 2% and 105 **±** 3% at pH 8.08 and 7.54, respectively) previously incorporated was depurated with a relatively short biological half-life ($Tb_{1/2}$ = 44 ± 12 and 55 ± 16 d at pH 8.08 and 7.54, respectively).

At ambient pH level, the gills displayed the highest activities with up to 3000 Bq g^{-1} wet weight (ww) and a CF of ~ 14 000 at the end of the uptake phase (14 d; Fig. 2). After only 7 days of exposure, 54 % and 22 % of the $i^{203}Hg$ whole body burden were found in the gills and the remaining tissues (including the skin), respectively (Table 2 and Fig. S3). After 14 days of exposure, these proportions were slightly lower, with 43 % and 16 % respectively, whereas the respective $i^{203}Hg$ concentrations in both compartments increased (Fig. 2 and S3). At the same time, the $i^{203}Hg$ activities and loads in the digestive gland and the digestive tract significantly increased during both the uptake and depuration periods; for the digestive gland, the $i^{203}Hg$ activities (and % with respect to the whole body activity) were 161 ± 53 Bq g^{-1} ww (11.9 ± 1.1%), 488 ± 211 Bq g^{-1} ww (14.5 ± 3.4%) at day 7 and 14 of the uptake phase respectively, and 653 ± 456 Bq g^{-1} ww (20.7 ± 5.2%) at day 21 of the depuration period. For the digestive tract, the activities (and the %) were ~ 70 Bq g^{-1} ww (3%), ~ 200 Bq g^{-1} ww (10%), ~ 230 Bq g^{-1} ww (6.5%), respectively. It is worth noted that muscular tissues (including mantle muscles, tentacles and arms) accounted for about 10% of the total $i^{203}Hg$ load, regardless of sampling time, despite their

very low activities (*i.e*. < 70 Bq g^{-1} ww). The branchial hearts, the optic lobes and the beak presented very low $i^{203}Hg$ activities with no significant change throughout the experiment course. Finally, the pH had no significant effect on the tissue distribution of accumulated $i^{203}Hg$.

Exposure to $Me^{203}Hg$ through trophic pathway

Despite sand goby and ditch shrimp were contaminated using $Me^{203}Hg$ radiolabelled food (fish pellets and brine shrimp), the analyses of the ^{203}Hg speciation in prey demonstrated that 82 ± 4% and only 30 ± 22% of the total ^{203}Hg amount were found under methylated form in the fish and shrimp, respectively. This implied that shrimp contained a large fraction of $i^{203}Hg$ compared to $Me^{203}Hg$ contrasting to fish that was mainly a source of $Me^{203}Hg$ for the cuttlefish in our experimental conditions.

Regardless of the experimental conditions, the depuration kinetics of dietary ^{203}Hg were best fitted to a mono-exponential model, suggesting that all the ^{203}Hg contained in each prey was assimilated (Fig. 3, Table 1). However, the loss kinetics of the radiotracer contrasted with respect to the prey type with a calculated ^{203}Hg $Tb_{1/2}$ of 25 ± 14 days for cuttlefish fed with shrimp at pH 8.08 and a $Tb_{1/2}$ that tends to infinity for cuttlefish fed with fish whether at pH 8.08 or at pH 7.54.

At ambient pH conditions (*i.e*. 8.08), the study of the ^{203}Hg organotropism revealed that the digestive gland contained the major fraction of the total ^{203}Hg body burden (72 ± 12%), high above the fraction values found in the remaining tissues, the mantle and the digestive tract (all below 10%) in shrimp-fed cuttlefish (Table 3). In contrast, cuttlefish contaminated with fish as a food source displayed similar proportions of ^{203}Hg in the digestive gland and digestive tract with 34 ± 10% and 32 ± 9%, respectively. After 21 days of depuration, the fraction of ^{203}Hg found in the digestive gland significantly decreased in the shrimp-fed cuttlefish (*i.e*. from 72% to 34%), whereas those in mantle and the remaining tissues increased from 7% to 22% and from 9% to 21%, respectively. These changes of loads between day 4 and day 21 were congruent with a 75% decrease of ^{203}Hg activity in the digestive gland (Fig. 2), decreasing from 1012 ± 317 Bq g^{-1} ww to 247 ± 96 Bq g^{-1} ww while the activities in the mantle and the

remaining tissues increased (from 20 ± 21 Bq g^{-1} to 48 ± 28 Bq g^{-1} and from 23 ± 19 Bq g^{-1} to 35 ± 19 Bq g^{-1}, respectively). In fish-fed cuttlefish, the fraction of the whole body ^{203}Hg found in the digestive gland, and to a lesser extent in the digestive tract, decreased all along the depuration period (*i.e*. from 34% to 8% and from 32% to 21%, at day 4 and day 21, respectively; Table 3). In contrast, the fractions found in muscular tissues (*viz.* mantle, tentacles, and arms) and the remaining tissues increased from 12% to 39% and from 12% to 25%, respectively. Consistently, the ^{203}Hg activity in the digestive gland tended to decrease from 280 ± 146 Bq g^{-1} ww at day 4 to 195 ± 181 Bq g^{-1} ww at day 21, whereas activity increased from 13 ± 4 Bq g^{-1} ww and 11 ± 3 Bq g^{-1} ww at day 4 to 85 ± 38 Bq g^{-1} ww and 70 ± 32 Bq g^{-1} ww at day 21 in the mantle and tentacles and arms, respectively. It is worth noting that the gills activity distribution and concentrations were constant regardless of the pH conditions. The other dissected tissues (*i.e*. branchial heart, optic lobes, beak) had low activities all along the experimental course. Finally, similarly to the experiment with dissolved Hg, pH did not significantly influence the tissue distribution of dietary accumulated Hg.

Bioaccumulation model

The kinetic parameters obtained from seawater and food experiments were used to feed a bioaccumulation model allowing an assessment of the relative contribution of each exposure pathway on total Hg bioaccumulation in juveniles of *Sepia officinalis*. Here, we applied this bioaccumulation model considering 1) a constant total dissolved iHg concentration in seawater of 1 x 10^{-3} ng mL^{-1} as measured by Cossa and Noël (1987), 2) fixed Hg concentrations in food of Cf = 6 ng g^{-1} fresh weight for ditch shrimp (data not shown) and Cf = 20 ng g^{-1} fresh weight for sand goby (Guimarães *et al.*, 2012) and 3) varying proportions of shrimp *vs*. fish in the diet and varying ingestion rate in accordance to the biology of the cuttlefish at three juvenile stages, *i.e*. the newly hatched, one-month-old and three-month-old juvenile cuttlefish. We also assume that the kinetic parameters remained constant regardless of exposure concentrations and within the range of these first months of juvenile life. Thus, the contribution from seawater and food (*i.e*. fish and shrimp) were calculated for three typical “stage”

scenarios: a newly hatched cuttlefish that fed mostly on shrimp with a IR of 0.50 g g^{-1} d^{-1}, a one-month old juvenile that fed on a mix of shrimp and fish (55 – 45%) with a decreasing IR of 0.35 g g^{-1} d^{-1} and three-months-old cuttlefish feeding mostly on fish with an IR of 0.10 g g^{-1} d^{-1} (Pinczon du Sel *et al.*, 2000) (Fig. 4). In all these three scenarios, the contribution of seawater never exceeded 2.3% of the total bioaccumulated Hg. Concerning the food type, shrimp contribute to 28.2% of the Hg bioaccumulation in newly hatched juveniles but decreased to 2.5% and 0.5% as fish contributions increased to 97.0% and 98.5% when the juvenile grows and changes its trophic regime.

Discussion

Food is the main source of total Hg for the cephalopods (see Penicaud *et al.,* 2017 for review). The contribution of dissolved Hg in seawater tends, however, to be overlooked in field studies while the coastal species might be subjected to local Hg contamination. In addition, the Hg transfer from food to cephalopods was mainly based on the hypothesis that prey mainly contain MeHg and/or iHg was not assimilated or retained. Thus, this lack of knowledge on the Hg accumulation dynamic in this class of animals exposed to both waterborne and dietary routes prevent to calculate each pathways contribution and estimate the size effect of environmental factors (*e.g*. prey type and seawater pCO_2) on the Hg bioaccumulation. Here, the Hg bioaccumulation capacity of cuttlefish juvenile was assessed by delineating the biokinetics of dissolved and dietary ^{203}Hg. The influence of prey (shrimp *vs.* fish; iHg/MeHg fractions they display) was tested as a major factor driving the assimilation efficiency and retention of Hg (*e.g*. Ponce and Bloom, 1991; Laporte *et al.*, 1997; Gworek *et al.*, 2016; Metian *et al.*, 2020). In addition, the increasing pCO_2 was considered as it could affect the animal metabolism, the dissolved metal bioconcentration (Lacoue-Labarthe *et al.,* 2009, 2011) and the assimilation through modulated digestive physiology (Melzner *et al.*, 2020).

Our results showed that the whole-body uptake kinetics of dissolved i^{203}Hg and the calculated whole-body CF_{ss} (709 ± 54 at pH 8.08) were in the same order of magnitude as a previous study on hatchlings

(480 ± 150; Lacoue-Labarthe *et al.*, 2009), confirming a relatively high bioconcentration efficiency of dissolved iHg in this species. At the end of the exposure period, the organisms were placed in non-contaminating conditions and the depuration kinetic parameters were determined for both species. The absorption efficiency A_0 (96% at pH 8.08) was comparable and the $Tb_{1/2}$ (44 days at pH 8.08) was slightly higher than this previous study (A_0 = 95% and $Tb_{1/2}$ = 17 days; Lacoue-Labarthe *et al.*, 2009). The slight differences of the values of the kinetics parameters for whole organisms between both studies could be partly explained by the age difference of the cuttlefish (*i.e*. 2 months old juveniles in the present study *vs*. newly hatched juveniles in Lacoue-Labarthe *et al.*, 2009 investigation).

When considering the different tissues, most of the accumulated $i^{203}Hg$ was found in the gills all along the uptake phase, and in the remaining tissues that include the skin (up to 58% and 22% of the total Hg load, respectively; Table 2). These tissues are in direct contact with seawater and therefore play a major role in the intake of waterborne trace elements including Hg (Bustamante *et al.*, 2006b). In fish, the uptake across the skin or oral epithelia is limited due to significant skin thickness, low surface area and limited blood perfusion (Pereira *et al.*, 2019). In contrast, cuttlefish skin is noticeably thinner than in fish, is quite permeable to oxygen and allows ammonia excretion (Birk *et al.*, 2018). Skin thus might not be excluded as a trace element absorption pathway, also as cuttlefish burrow into sediment during daylight, allowing trace elements dissolved in the interstitial seawater to be incorporated into the organism (Bustamante *et al.*, 2004).

The increase of Hg activities and loads in the digestive gland during the uptake as well as the loss phases highlights the Hg transfer to this organ in relation to its key role in trace element detoxification (Penicaud *et al.*, 2017). Similarly, 87% and 76% of the whole body burdens of cadmium (Cd) and zinc (Zn), respectively, have been mainly found in the cuttlefish digestive gland following dissolved metal exposure and depuration (Bustamante *et al.*, 2002). Investigations on trace element detoxification in the digestive gland revealed that metallothionein-like proteins' were involved in the detoxification of silver (Ag) and copper (Cu) whereas Cd and Zn seems to mainly bind high (>70kDa) and low (<4kDa) molecular weight proteins (Bustamante *et al.*, 2006a). Moreover, metal-rich spherules are present in

the basal cells of the digestive gland of *Sepia officinalis* (Martoja and Marcaillou, 1993; Costa *et al.*, 2014). Martoja and Marcaillou (1993) hypothesized that these spherules contain cysteine-rich proteins (*i.e*. metallothionein-like proteins) to which several metals have a high affinity. Cysteine is considered as the primary target of iHg which has a high affinity for thiol residues (Manceau *et al.*, 2019; Ajsuvakova *et al.*, 2020). However, such detoxification mechanisms deserve further investigations in cephalopods.

The distribution of dissolved $i^{203}Hg$ was previously determined only on a very limited number of tissues (*i.e*. digestive gland, cuttlebone and the remaining tissues) given the very small size of the cuttlefish (newly hatched individuals; Lacoue-Labarthe *et al.*, 2009). Hg was mainly stored in the remaining tissues (up to 80% of the total Hg load), which are mainly composed of muscles, but also include the skin and the respiratory organs (*i.e*. gills). Lacoue-Labarthe *et al.,* (2009) suggested that iHg was mainly stored in the muscles as it has a strong affinity for the sulfhydryl groups of muscular proteins (Bloom, 1992; Bustamante *et al.*, 2006b). Nevertheless, by separating more accurately the different organs in our larger cuttlefish, we demonstrated a limited redistribution of iHg toward muscular tissues (*i.e*. mantle, tentacles and arms ~ 10%) compared to the gills (~ 45%) and the digestive gland (~ 20%). This highlights the need to consider the different tissues separately to delineate their role in metal metabolism.

When the non-contaminating conditions were restored and depuration kinetics of $i^{203}Hg$ were followed, it is noteworthy that the radiotracer activity in the gills remained constant. This contrasts with the Hg efficient elimination from the gills reported in other marine organisms such as the white seabream *Diplodus sargus* (Pereira et al., 2015) or the king scallop *Pecten maximus* (Metian *et al.*, 2008). In the latter species, more than 70% of accumulated $i^{203}Hg$ in the gills was lost after 3 weeks of depuration. Our result suggests that the primary organ for waterborne Hg incorporation would retain Hg very efficiently in cuttlefish. In fact, Hg could be tightly adsorbed onto the high gill's external surface or efficiently bound to the gill's cell compounds, such as sulfhydryl groups of metalloproteins or glutathione (Viarengo *et al.*, 1997; Metian *et al.*, 2008). Alternatively, a slow Hg loss might obscure a

constant supply of Hg through the blood from the digestive gland and/or from the other tissues whose concentrations decreased during the loss period.

Concerning the trophic transfer experiments, the main result is the strong effect of the food type (fish *vs.* shrimp) on the whole-body depuration kinetics. In this study, the whole Hg content in fish and shrimp has been assimilated by cuttlefish while the depuration was strongly dependent on the ingested prey-type, with k_e ranged from 0.002 (fish) to 0.028 (shrimp; Table 1). Consequently, the Hg retention capacities differed: $Tb_{1/2}$ in whole cuttlefish was relatively shorth in shrimp-fed cuttlefish (25 days) and extremely long in fish fed animals (not different form infinity). We suggest here that the variation of these kinetic parameters is mainly resulting from the different proportion of Hg species in the prey. The proportion of MeHg over the total ^{203}Hg accumulated was indeed much higher in fish (>80%) than in shrimp (about only 30%). Other factors, not investigated here, such as tissular and subcellular distribution driving metal bioaccessibility could also play a key role on trace element assimilation (Ni *et al.*, 2000; Pouil *et al.*, 2016). Moreover, differences in trophic transfer of iHg and MeHg has been previously seen in copepods, in mussels and in fish (Trudel and Rasmussen, 1997; Wang and Wong, 2003; Feng *et al.*, 2015; Lee and Fisher, 2017; Pinzone *et al.*, 2022), especially with respect to the lower excretion rates of organomercurial species when compared to the iHg observed in fish (Trudel and Rasmussen, 1997; Feng *et al.*, 2015). Thus, our results strongly suggest that the more abundant iHg contained in the shrimp is rapidly eliminated contributing to the lower $Tb_{1/2}$ of the total assimilated ^{203}Hg when compared to the long Hg retention in fish-fed cuttlefish.

Regarding ^{203}Hg distribution among tissues, most of the Hg from enriched shrimp prey was rapidly taken up by the digestive gland, which contained >70% of the whole-body activity at day 4. This substantiates the key role of the digestive gland in trapping the inorganic Hg contained in shrimp, through the induction of chelating proteins as reported in previous works (Rodrigo and Costa, 2017; Penicaud *et al*., 2017). At day 21, the digestive gland contained about 40% of the whole-body activity

and 65% of its initial concentration (Fig. 2) showing the digestive gland depurates efficiently iHg. By comparison, the $Tb_{1/2}$ of dietary iHg is shorter than that of waterborne iHg (*i.e*. $Tb_{1/2}$ = 25 and 44 days, respectively), as observed in the fish sweetlips (Wang and Wong, 2003). These differences are congruent with the fact that dietary iHg was directly trapped by the digestive gland during digestive processes whereas waterborne iHg has to be transferred over time from tissues of absorption (*i.e*. gills and skin) towards the digestive gland, before being eliminated.

The remaining tissues contain about 10% of the Hg whole body burden at 4 days, which increased until 25% at 21 days. Such a high proportion could be imputed by the presence of eyes, muscular tissues (*e.g*. buccal mass – see below), and the kidneys known to highly concentrate iHg (Raimundo *et al.*, 2014). Cuttlefish fed with radiolabelled fish had most of the ^{203}Hg load in their digestive gland and digestive tract on day 4 (*i.e*. 34.2% and 32.1% for pH 8.08 and 40.8% and 30.7% for pH 7.54, respectively). They then showed an increase of the radiotracer distribution from day 4 to day 21 in muscular tissues (*i.e*. mantle, tentacles and arms and remaining tissues), as seen to a lesser extent in the shrimp-fed individuals. This was consistent with a transitory metal care by the digestive organs before a transfer and binding of MeHg to muscle proteins as previously mentioned. However, the lower Hg proportion in muscular tissues at day 21 in cuttlefish fed with shrimp (*i.e*. 49.4%) than in cuttlefish fed with fish (*i.e*. 64.2%) suggests that, as for waterborne metal, the iHg contained in the shrimp was poorly transferred and stored in the muscular tissues. Instead, this result supports that iHg was also retained by the digestive gland and subsequently depurated.

Cuttlefish fed with radiolabelled shrimp showed an increase of the radiotracer in the digestive tract from day 4 to day 21, which was not observed in the cuttlefish fed with fish. As a consequence of a different Hg speciation between the foods, this result suggests that the digestive tract plays a key role in iHg excretion. Nonetheless, there is still a relatively high Hg load in the digestive tract suggesting a high affinity of MeHg with this tissue. Both these observations question the potential role of the intestine and its microbiome in the accumulation and possible transformation of Hg in the digestive tract (Li *et al.*, 2019). Nevertheless, the Hg activity tended to increase in all analysed tissues (except

the digestive gland and digestive tract), which might partly be attributable to MeHg being transferred from the digestive gland to all tissues and accumulate according to its affinity related to the tissue composition. After 21 days, more than 95% of the initial activity remained in the cuttlefish fed with fish demonstrating a limited elimination of MeHg.

Finally, ^{203}Hg activities were undetectable in the beak, which is usually used to trace Hg contamination in cephalopods (Queirós *et al.*, 2020), likely due to a low incorporation rate. In contrast, the optic lobes activities were similar to the mantle following the trophic Hg exposure, confirming that nervous tissues are target organ for MeHg accumulation in cephalopods (Minet *et al*., 2021).

In this study, the non-effect of pH/pCO_2 on the Hg bioaccumulation contrasted those reported for different marine organisms. For instance, under elevated pCO_2 Hg concentrations decreased in the copepod *Tigriopus japonicus* exposed to dissolved iHg and in the meagre *Argyrosomus regius* fed with enriched MeHg food (Li *et al.*, 2017; Sampaio *et al.*, 2018). The similar waterborne iHg CF_{ss}, k_u and k_e, whatever the pH, suggests that despite the increase of H^+ in acidified conditions, protons did not significantly compete influx pathway with Hg^{2+} to limit the bioconcentration efficiencies as hypothesized by Li and collaborators (2007). In addition, elevated upregulated branchial acid-base and ion regulatory processes by elevated pCO_2 (Melzner *et al.*, 2020) did not affect the iHg absorption efficiency although iHg proportion in gills of cuttlefish exposed to dissolved iHg at pH 7.54 compared to pH 8.08 tended to be slightly higher. Wang and Wong (2003) indicated that Hg uptake was primarily a Freundlich absorption type dominated by passive diffusion or a facilitated transport process, suggesting that iHg might not be mainly influenced by ionic activities. Then, the seawater pH/pCO_2 can impact intestinal cationic regulation, (Hu *et al.*, 2017), digestive processes and assimilation efficiencies (Melzner *et al*., 2020). Here, the AE of the MeHg in fish prey have not been affected by elevated pCO_2 consistently with the fact that the Hg organic form does not favour its passage through ion channels. In addition, these results did not support decreasing diffusion for the organic and metal complex within

the membrane, through increased protonation of phospholipid by the lowering pH (Boullemant *et al.*, 2009; Li *et al.*, 2017). Finally, cephalopod like fish may have the ability to self-regulate pH shifts in their digestive tract explaining that ocean acidification will not affect the trophic transfer of metals in these organisms (Jacob *et al.*, 2017).

Using the kinetic parameters experimentally determined in this study, the calculation of the route contribution demonstrates that food is the predominant pathway for Hg bioaccumulation in juvenile cuttlefish, as previously considered (Chouvelon *et al.* 2011; Penicaud *et al.*, 2017). We have considered three "case studies" of diet and ingestion rate changing with age, based on the known ecology and biology of *Sepia officinalis.* Newly hatched juveniles preferentially consume small invertebrates such as shrimps (*i.e*. 95%), with a high ingestion rate to fill their energetic needs (Darmaillacq *et al.*, 2004). In these crustaceans, Hg is mainly under the inorganic form, which is easily eliminated (see above). In this group, the few consumed fish (*i.e*. 5%), assuming their total concentration as MeHg, represent most of the Hg accumulated (*i.e*. 69.5%, Fig. 4). During the growing phase, due to their opportunistic behaviour and flexible diet and despite a decreasing ingestion rate with age, juveniles consume larger prey and include more fish in their diet (Pinczon du Sel *et al.*, 2000). Thus, fish contribute to 97% and 98.5% of the accumulated Hg in the juvenile and three-months-old juvenile cuttlefish. As previously shown, the $Tb_{1/2}$ of the dietary MeHg in cuttlefish is extremely long (not significantly different from infinity) and would deserve a higher concern about its toxicity on this cephalopod species. Finally, this shows that effort should continue to limit Hg contamination of the marine environment as it efficiently biomagnifies along trophic webs as soon as methylated, raising important questions about environmental concerns and human health risk.

Conclusion

This paper brought the kinetic parameters of dissolved iHg and trophic iHg/MeHg in cuttlefish exposed to environmentally realistic conditions with respect to their good health status maintained during

experiment and the use of natural prey. The results showed that iHg, whatever the source, is rapidly taken in charge by the digestive gland, a key organ for metal detoxification, before being eliminated. Contrasting to this, dietary MeHg is transferred to other tissues, mainly the muscular tissues and is infinitely retained, making of the MeHg contained in prey the main source of Hg contamination for cuttlefish. Nonetheless, the significant amount of iHg and MeHg found in the digestive tract raises the potential implication of the microbiome in methylation and/or demethylation processes of the dietary Hg. Surprisingly, the pCO_2 does not increase nor alleviate the Hg bioaccumulation efficiency. These results open the question of the Hg toxicity on the cuttlefish physiology and underline the key role of cephalopod in the Hg transfer along the food chain considering their pivotal place in trophic webs.

Acknowledgments

This work is a contribution to the MERCy project funded by *la Fondation pour la Recherche sur la Biodiversité* and the *Ministère de la Transition Ecologique et Solidaire*. The *Région Nouvelle Aquitaine* is acknowledged for its support to the PhD grant to AM through the EXPO project. The Institut Universitaire de France (IUF) is acknowledged for its support to PB as a Senior Member. AT, SA, FO, MM, and PWS are grateful for the support provided to the Environment Laboratories by the government of the Principality of Monaco. This work benefitted from the French GDR "Aquatic Ecotoxicology" framework which aims at fostering stimulating scientific discussions and collaborations for more integrative approaches. Authors warmly thank Antoine and José Lacoue-Labarthe, Jérôme Fort, Rémy Guilloneau and Fernando Pedraza for their support during field sampling. This work benefitted from the French GDR "Aquatic Ecotoxicology" framework, which aims at fostering stimulating scientific discussions and collaborations for more integrative approaches.

References

Ajsuvakova OP, Tinkov AA, Aschner M, Rocha JBT, Michalke B, Skalnaya MG, Skalny AV, Butnariu M, Dadar M, Sarac I, Aaseth J, Bjørklund G. 2020. Sulfhydryl groups as targets of mercury toxicity. *Coord Chem Rev* 417: 213343.

Azemard S, Vassileva E. 2015. Determination of methylmercury in marine biota samples with advanced mercury analyzer: method validation. *Food Chem* 176: 367–375.

Belivermiş M, Besson M, Swarzenski P, Oberhänsli F, Taylor A, Metian M. 2020. Influence of pH on Pb accumulation in the blue mussel, *Mytilus edulis*. *Mar Pollut Bull* 156.

Benoit JM, Gilmour CC, Heyes A, Mason RP, Miller CL. 2002. Geochemical and Biological Controls over Methylmercury Production and Degradation in Aquatic Ecosystems. Biogeochemistry of Environmentally Important Trace Elements, American Chemical Society., 262–297.

Birk MA, Dymowska AK, Seibel BA. 2018. Do squid breathe through their skin? *J Exp Biol* 221: jeb185553.

Bisi T, Lepoint G, Azevedo A, Dorneles P, Flach L, Das K, Malm O, Lailson Brito J. 2012. Trophic relationships and mercury biomagnification in Brazilian tropical coastal food webs. *Ecol Indic* 18: 291–302.

Blanc A, Pinczon Du Sel G, Daguzan J. 1998. Habitat and diet of early stages of *Sepia officinalis* L. (Cephalopoda) in Morbihan Bay, France. *J Molluscan Stud* 64: 263–274.

Bloom NS. 1992. On the Chemical Form of Mercury in Edible Fish and Marine Invertebrate Tissue. *Can J Fish Aquat Sci*.

Boucaud-Camou E, Boismery J. 1991. The Migrations of the Cuttlefish (*Sepia officinalis* L.) in the English Channel. *Seiche Actes Prem Symp Int Sur Seiche Caen 1-3 June 1989* 141–151.

Boullemant A, Lavoie M, Fortin C, Campbell PGC. 2009. Uptake of Hydrophobic Metal Complexes by Three Freshwater Algae: Unexpected Influence of pH. *Environ Sci Technol* 43: 3308–3314.

Bustamante P, Teyssié J-L, Fowler SW, Cotret O, Danis B, Warnau M. 2002. Biokinetics of cadmium and zinc accumulation and depuration at different stages in the life cycle of the cuttlefish *Sepia officinalis*. *Mar Ecol Prog Ser* 231: 167–177.

Bustamante P, Teyssié J-L, Danis B, Fowler SW, Miramand P, Cotret O, Warnau M. 2004. Uptake,

transfer and distribution of silver and cobalt in tissues of the common cuttlefish *Sepia officinalis* at different stages of its life cycle. *Mar Ecol Prog Ser* 269: 185–195.

Bustamante P, Bertrand M, Boucaud-Camou E, Miramand P. 2006a. Subcellular distribution of Ag, Cd, Co, Cu, Fe, Mn, Pb and Zn in the digestive gland of the common cuttlefish *Sepia officinalis*. *J Shellfish Res* 25: 987–993.

Bustamante P, Lahaye V, Durnez C, Churlaud C, Caurant F. 2006b. Total and organic Hg concentrations in cephalopods from the North East Atlantic waters: influence of geographical origin and feeding ecology. *Sci Total Environ* 368: 585–596.

Carravieri A, Cherel Y, Blévin P, Brault-Favrou M, Chastel O, Bustamante P. 2014. Mercury exposure in a large subantarctic avian community. *Environ Pollut 1987* 190: 51–57.

Chouvelon T, Spitz J, Cherel Y, Caurant F, Sirmel R, Mèndez-Fernandez P, Bustamante P. 2011. Inter-specific and ontogenic differences in $\delta^{13}C$ and $\delta^{15}N$ values and Hg and Cd concentrations in cephalopods. *Mar Ecol Prog Ser* 433: 107–120.

Chouvelon T, Cresson P, Bouchoucha M, Brach-Papa C, Bustamante P, Crochet S, Fabri M-C, Marco-Miralles F, Thomas B, Knoery J. 2018. Oligotrophy as a major driver of mercury bioaccumulation in marine medium-to high-trophic level consumers: A marine ecosystem-comparative study. *Environ Pollut* 233: 844–854.

Cossa D, Noël J. 1987. Concentrations of mercury in near shore surface waters of the bay of Biscay and in the Gironde Estuary. *Mar Chem* 20: 389–396.

Costa PM, Rodrigo AP, Costa MH. 2014. Microstructural and histochemical advances on the digestive gland of the common cuttlefish, *Sepia officinalis* L. *Zoomorphology* 133: 59–69.

Darmaillacq A-S, Chichery R, Poirier R, Dickel L. 2004. Effect of early feeding experience on subsequent prey preference by cuttlefish, *Sepia officinalis*. *Dev Psychobiol* 45: 239–244.

Dorey N, Melzner F, Martin S, Oberhänsli F, Teyssié J-L, Bustamante P, Gattuso J-P, Lacoue-Labarthe T. 2013. Ocean acidification and temperature rise: effects on calcification during early development of the cuttlefish *Sepia officinalis*. *Mar Biol* 160: 2007–2022.

Feng C, Pedrero Z, Gentès S, Barre J, Renedo M, Tessier E, Berail S, Maury-Brachet R, Mesmer-Dudons N, Baudrimont M, Legeay A, Maurice L, Gonzalez P, Amouroux D. 2015. Specific Pathways of

Dietary Methylmercury and Inorganic Mercury Determined by Mercury Speciation and Isotopic Composition in Zebrafish (*Danio rerio*). *Environ Sci Technol* 49: 12984–12993.

Gattuso J-P, Hansson L. 2011. Ocean Acidification, Oxfod University Press, Oxford, UK, 347 p.

Gattuso J-P, Epitalon J-M, Lavigne H, Orr J, Gentili B, Hagens M, Hofmann A, Mueller J-D, Proye A, Rae J, Soetaert K. 2021. seacarb: Seawater Carbonate Chemistry. R package version 3.2.16. https://CRAN.R-project.org/package=seacarb

Guimarães L, Medina MH, Guilhermino L. 2012. Health status of Pomatoschistus microps populations in relation to pollution and natural stressors: implications for ecological risk assessment. *Biomark Biochem Indic Expo Response Susceptibility Chem* 17: 62–77.

Gworek B, Bemowska-Kałabun O, Kijeńska M, Wrzosek-Jakubowska J. 2016. Mercury in Marine and Oceanic Waters—a Review. *Water Air Soil Pollut* 227.

Hu M, Tseng Y-C, Su Y-H, Lein E, Lee H-G, Lee J-R, Dupont S, Stumpp M. 2017. Variability in larval gut pH regulation defines sensitivity to ocean acidification in six species of the Ambulacraria superphylum. *Proc R Soc B Biol Sci* 284: 20171066.

Jackson GD, Bustamante P, Cherel Y, Fulton EA, Grist E p.m, Jackson CH, Nichols PD, Pethybridge H, Phillips K, Ward RD, Xavier JC. 2006. Applying new tools to cephalopod trophic dynamics and ecology: perspectives from the Southern Ocean Cephalopod Workshop, February 2–3, 2006. *Rev Fish Biol Fish* 17: 79–99.

Jacob H, Pouil S, Lecchini D, Oberhänsli F, Swarzenski P, Metian M. 2017. Trophic transfer of essential elements in the clownfish *Amphiprion ocellaris* in the context of ocean acidification. *PLoS One* 12: e0174344.

Jiskra M, Heimbürger-Boavida L-E, Desgranges M-M, Petrova MV, Dufour A, Ferreira-Araujo B, Masbou J, Chmeleff J, Thyssen M, Point D, Sonke JE. 2021. Mercury stable isotopes constrain atmospheric sources to the ocean. *Nature* 597: 678–682.

Kroeker KJ, Kordas RL, Crim RN, Singh GG. 2010. Meta-analysis reveals negative yet variable effects of ocean acidification on marine organisms. *Ecol Lett* 13: 1419–1434.

Lacoue-Labarthe T, Warnau M, Oberhänsli F, Teyssié J-L, Bustamante P. 2009. Bioaccumulation of inorganic Hg by the juvenile cuttlefish *Sepia officinalis* exposed to ^{203}Hg radiolabelled seawater and

food. *Aquat Biol* 6: 91–98.

Lacoue-Labarthe T, Réveillac E, Oberhänsli F, Teyssié JL, Jeffree R, Gattuso JP. 2011. Effects of ocean acidification on trace element accumulation in the early-life stages of squid *Loligo vulgaris*. *Aquat Toxicol* 105: 166–176.

Laporte JM, Truchot JP, Ribeyre F, Boudou A. 1997. Combined effects of water pH and salinity on the bioaccumulation of inorganic mercury and methylmercury in the shore crab *Carcinus maenas*. *Mar Pollut Bull* 34: 880–893.

Lee C-S, Fisher NS. 2017. Bioaccumulation of methylmercury in a marine copepod. *Environ Toxicol Chem* 36: 1287–1293.

Li H, Lin X, Zhao J, Cui L, Wang L, Gao Y, Li B, Chen C, Li Y-F. 2019. Intestinal Methylation and Demethylation of Mercury. *Bull Environ Contam Toxicol* 102: 597–604.

Li Y, Wang W-X, Wang M. 2017. Alleviation of mercury toxicity to a marine copepod under multigenerational exposure by ocean acidification. *Sci Rep* 7: 324.

Manceau A, Bustamante P, Haouz A, Bourdineaud JP, Gonzalez-Rey M, Lemouchi C, Gautier-Luneau I, Geertsen V, Barruet E, Rovezzi M, Glatzel P, Pin S. 2019. Mercury(II) Binding to Metallothionein in *Mytilus edulis* revealed by High Energy-Resolution XANES Spectroscopy. *Chemistry - A European Journal* 25: 997–1009.

Martoja M, Marcaillou C. 1993. Localisation cytologique du cuivre et de quelques autres métaux dans la glande digestive de la seiche, *Sepia officinalis* L (Mollusque Céphalopode). *Can J Fish Aquat Sci*.

Melzner F, Mark FC, Seibel BA, Tomanek L. 2020. Ocean Acidification and Coastal Marine Invertebrates: Tracking CO_2 Effects from Seawater to the Cell. *Annu Rev Mar Sci* 12: 499–523.

Metian M, Warnau M, Cosson RP, Oberhänsli F, Bustamante P. 2008. Bioaccumulation and detoxification processes of Hg in the king scallop *Pecten maximus*: field and laboratory investigations. *Aquat Toxicol* 90: 204–213.

Metian M, Pouil S, Dupuy C, Teyssié J-L, Warnau M, Bustamante P. 2020. Influence of food (ciliate and phytoplankton) on the trophic transfer of inorganic and methyl-mercury in the Pacific cupped oyster *Crassostrea gigas*. *Environ Pollut* 257: 113503.

Millero F, Woosley R, DiTrolio B, Waters J. 2009. Effect of Ocean Acidification on the Speciation of

Metals in Seawater. *Oceanography* 22: 72–85.

Minet A, Manceau A, Valada-Mennuni A, Brault-Favrou M, Churlaud C, Fort J, Nguyen T, Spitz J, Bustamante P, Lacoue-Labarthe T. 2021. Mercury in the tissues of five cephalopods species: First data on the nervous system. *Sci Total Environ* 759: 143907.

Ni I-H, Wang W-X, Tam YK. 2000. Transfer of Cd, Cr and Zn from zooplankton prey to mudskipper Periophthalmus cantonensis and glassy Ambassis urotaenia fishes. *Mar Ecol Prog Ser* 194: 203–210.

Nilsson GE, Dixson DL, Domenici P, McCormick MI, Sørensen C, Watson S-A, Munday PL. 2012. Near-future carbon dioxide levels alter fish behaviour by interfering with neurotransmitter function. *Nature Clim Change* 2: 201–204.

Pascal P-Y, Fleeger JW, Galvez F, Carman KR. 2010. The toxicological interaction between ocean acidity and metals in coastal meiobenthic copepods. *Mar Pollut Bull* 60: 2201–2208.

Penicaud V, Lacoue-Labarthe T, Bustamante P. 2017. Metal bioaccumulation and detoxification processes in cephalopods: A review. *Environ Res* 155: 123–133.

Pereira P, Korbas M, Pereira V, Cappello T, Maisano M, Canário J, Almeida A, Pacheco M. 2019. A multidimensional concept for mercury neuronal and sensory toxicity in fish - From toxicokinetics and biochemistry to morphometry and behavior. *Biochim Biophys Acta BBA - Gen Subj* 1863: 129298.

Pinczon du Sel G, Blanc A, Daguzan J. 2000. The diet of the cuttlefish *Sepia officinalis* L. (mollusca: cephalopoda) during its life cycle in the Northern Bay of Biscay (France). *Aquat Sci* 62: 167–178.

Pinzone M, Cransveld A, De Boeck G, Shrivastava J, Tessier E, Bérail S, Schnitzler JG, Amouroux D, Das K. 2022. Dynamics of Dietary Mercury Determined by Mercury Speciation and Isotopic Composition in *Dicentrarchus labrax*. *Front Environ Chem* 3: 767202.

Ponce RA, Bloom NS. 1991. Effect of pH on the bioaccumulation of low level, dissolved methylmercury by rainbow trout (*Oncorhynchus mykiss*). *Water Air Soil Pollut* 56: 631–640.

Pörtner HO, Farrell AP. 2008. Physiology and Climate Change. *Science* 322: 690–692.

Pouil S, Warnau M, Oberhänsli F, Teyssié J-L, Bustamante P, Metian M. 2016. Influence of food on the assimilation of essential elements (Co, Mn, and Zn) by turbot *Scophthalmus maximus*. *Mar Ecol Prog Ser* 550: 207–218.

Queirós JP, Bustamante P, Cherel Y, Coelho JP, Seco J, Roberts J, Pereira E, Xavier JC. 2020. Cephalopod beak sections used to trace mercury levels throughout the life of cephalopods: The giant warty squid *Moroteuthopsis longimana* as a case study. *Mar Environ Res* 161: 105049.

R. Core Team. 2019. R: A language and environment for statistical computing. R Foundation for Statistical Computing, Vienna, Austria. URL https://www.R-project.org/.

Raimundo J, Pereira P, Vale C, Canário J, Gaspar M. 2014. Relations between total mercury, methylmercury and selenium in five tissues of *Sepia officinalis* captured in the south Portuguese coast. *Chemosphere* 108: 190–196.

Ramaglia AC, de Castro LM, Augusto A. 2018. Effects of ocean acidification and salinity variations on the physiology of osmoregulating and osmoconforming crustaceans. *J Comp Physiol [B]* 188: 729–738.

Rodrigo AP, Costa PM. 2017. The Role of the Cephalopod Digestive Gland in the Storage and Detoxification of Marine Pollutants. *Front Physiol* 8: 232.

Rouleau C, Block M. 1997. Fast and high-yield synthesis of radioactive $CH_3{}^{203}Hg(II)$. *Appl Organomet Chem* 11: 751–753.

Sampaio E, Lopes AR, Francisco S, Paula JR, Pimentel M, Maulvault AL, Repolho T, Grilo TF, Pousão-Ferreira P, Marques A, Rosa R. 2018. Ocean acidification dampens physiological stress response to warming and contamination in a commercially-important fish (*Argyrosomus regius*). *Sci Total Environ* 618: 388–398.

Shi W, Zhao X, Han Y, Che Z, Chai X, Liu G. 2016. Ocean acidification increases cadmium accumulation in marine bivalves: a potential threat to seafood safety. *Sci Rep* 6: 20197.

Sonke JE, Teisserenc R, Heimbürger-Boavida L-E, Petrova MV, Marusczak N, Le Dantec T, Chupakov AV, Li C, Thackray CP, Sunderland EM, Tananaev N, Pokrovsky OS. 2018. Eurasian river spring flood observations support net Arctic Ocean mercury export to the atmosphere and Atlantic Ocean. *Proc Natl Acad Sci* 115: E11586–E11594.

Stockdale A, Tipping E, Lofts S, Mortimer RJG. 2016. Effect of Ocean Acidification on Organic and Inorganic Speciation of Trace Metals. *Environ Sci Technol* 50: 1906–1913.

Storelli MM, Garofalo R, Giungato D, Giacominelli-Stuffler R. 2010. Intake of essential and non-essential

elements from consumption of octopus, cuttlefish and squid. *Food Addit Contam Part B* 3: 14–18.

Stumpp M, Wren J, Melzner F, Thorndyke MC, Dupont ST. 2011. CO2 induced seawater acidification impacts sea urchin larval development I: Elevated metabolic rates decrease scope for growth and induce developmental delay. *Comp Biochem Physiol A Mol Integr Physiol* 160: 331–340.

Thomann RV. 1981. Equilibrium model of fate of microcontaminants in diverse aquatic food chains. *Can J Fish Aquat Sci* 38: 280–296.

Thomann RV, Mahony JD, Mueller R. 1995. Steady-state model of biota sediment accumulation factor for metals in two marine bivalves. *Environ Toxicol Chem Int J* 14: 1989–1998.

Trudel M, Rasmussen JB. 1997. Modeling the Elimination of Mercury by Fish. *Environ Sci Technol* 31: 1716–1722.

van der Velden S, Dempson JB, Evans MS, Muir DCG, Power M. 2013. Basal mercury concentrations and biomagnification rates in freshwater and marine food webs: effects on Arctic charr (*Salvelinus alpinus*) from eastern Canada. *Sci Total Environ* 444: 531–542.

Viarengo A, Ponzano E, Dondero F, Fabbri R. 1997. A simple spectrophotometric method for metallothionein evaluation in marine organisms: an application to Mediterranean and Antarctic molluscs. *Mar Environ Res* 44: 69–84.

Wang W, Wong R. 2003. Bioaccumulation kinetics and exposure pathways of inorganic mercury and methylmercury in a marine fish, the sweetlips *Plectorhinchus gibbosus*. *Mar Ecol Prog Ser* 261: 257–268.

Warnau M, Bustamante P. 2007. Radiotracer Techniques: A Unique Tool in Marine Ecotoxicological Studies. *Environ Bioindic* 2: 217–218.

Warnau M, Teyssié J-L, Fowler SW. 1996. Biokinetics of selected heavy metals and radionuclides in the common Mediterranean echinoid *Paracentrotus lividus*: sea water and food exposures. *Mar Ecol Prog Ser* 141: 83–94.

Whicker FW, Schultz V. 1982. Radioecology: nuclear energy and the environment. United States: CRC Press, Inc.

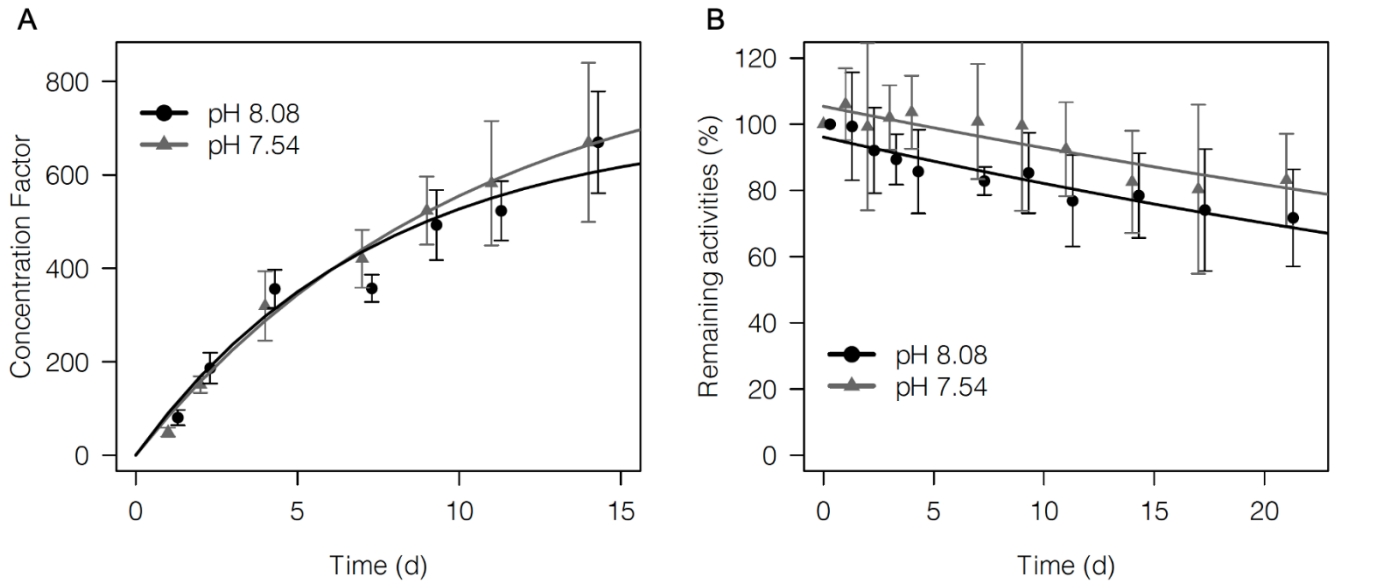

Fig. 1: A: Uptake kinetics expressed as Concentration Factors (mean ± SD) over time (in days) in juvenile common cuttlefish *Sepia officinalis* (n = 12 per group until day 7 and then n = 9) exposed for 2 weeks to dissolved $i^{203}Hg$ at two pHs. B: Loss kinetics of $i^{203}Hg$ in juvenile of cuttlefish (n = 6 per group) previously exposed to dissolved iHg for two weeks and then maintained for three weeks in depuration conditions, at two pHs.

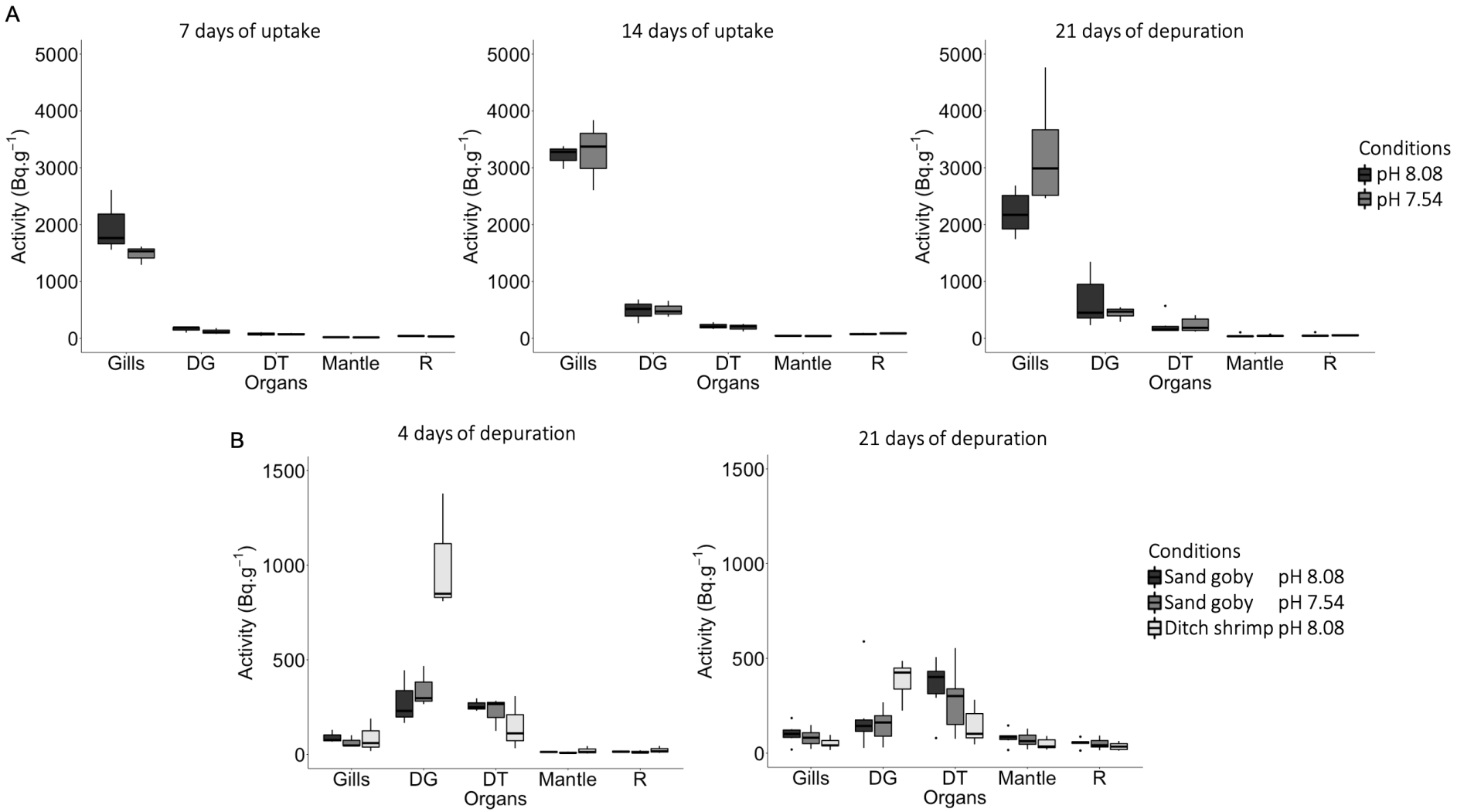

Fig. 2: Activity (in Bq g^{-1} wet weight) of ^{203}Hg in the main organs, that count for >90% of the accumulated Hg (see Table 2), of the common cuttlefish *Sepia officinalis* reared at two pHs (8.08 and 7.54) A) sampled at 7, 14 days of uptake and 21 days of depuration following dissolved $i^{203}Hg$ exposure and B) sampled after 4 and 21 d following a pulse chase feeding with $Me^{203}Hg$ radiolabelled fish (sand goby) and shrimp (ditch shrimp). DG = digestive gland, DT = digestive tract, R = remaining tissues. The whiskers indicate the standard deviation, the midline in each box indicates the median, upper and lower quartiles indicate 25% and 75% quartiles respectively and black dots are outliers.

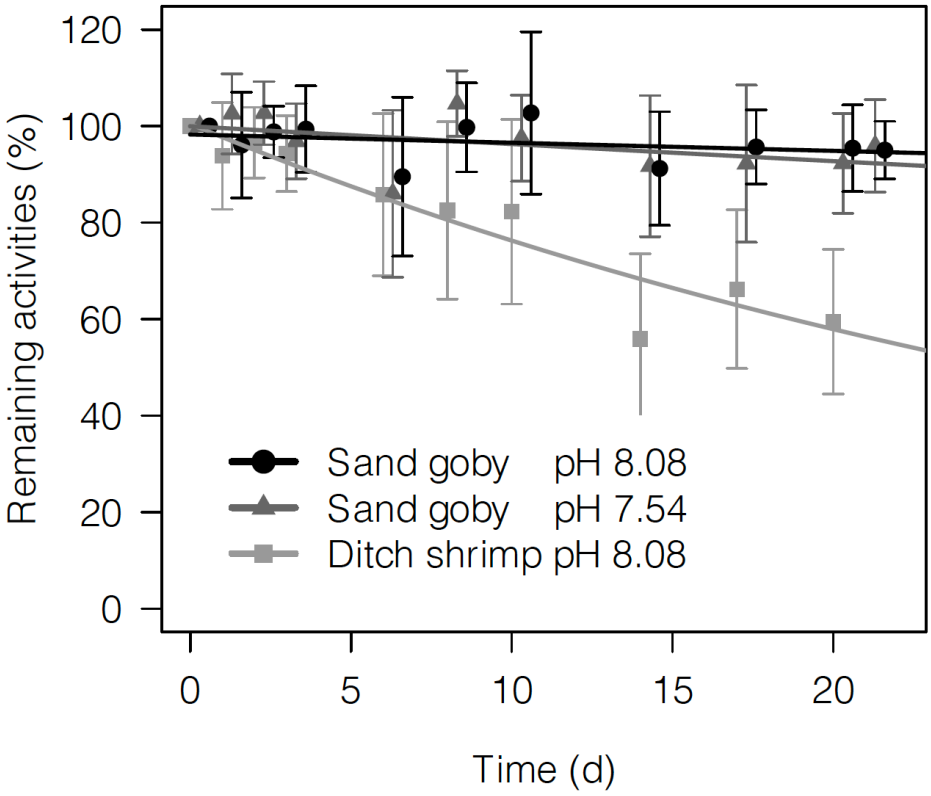

Fig. 3: Loss kinetics of ^{203}Hg (mean ± SD) in juvenile of the common cuttlefish *Sepia officinalis* (n = 12 per group until day 4, then n = 9 per group) contaminated by a pulse chase feeding on two types of prey (sand goby and ditch shrimp) previously radiolabelled with Me^{203}Hg. Cuttlefish fed on fish were also maintained at two pHs.

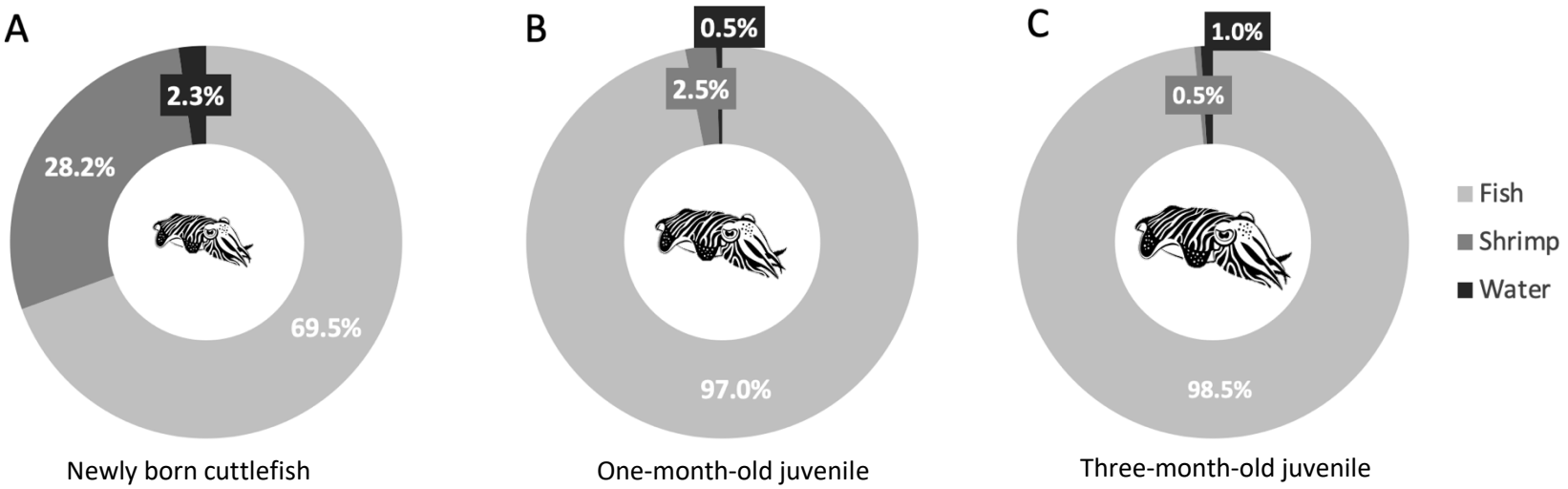

Fig. 4: Evolutive Hg contribution scenarios from food (fish and shrimp) and water. A: Newly born cuttlefish feeding with 95% of shrimp and 5% of fish with an IR=0.50. B: One-month-old juvenile cuttlefish feeding with 55% of shrimp and 45% of fish with an IR=0.35. Three-months-old juvenile cuttlefish feeding with 20% of shrimp and 80% of fish with an IR=0.10.

Table 1: Whole-body uptake and loss kinetic parameters of ^{203}Hg in whole common cuttlefish, *Sepia officinalis* following different exposure experiments: (1) individuals (n = 24) were exposed for 10 d to the radiotracer in seawater at two pH then (2) placed in depuration conditions for 21 d (n = 18); (3) individuals fed on radiolabelled fish (sand goby *Pomatoschistus minutus*) or shrimp (ditch shrimp *Palaemon varians*) were placed in depuration conditions at two pH for 21 d (n = 36). Uptake parameters—CF_{ss}: concentration factor at steady state (mean ± SD); k_u: uptake rate constant (d^{-1}). All loss kinetics followed a mono-exponential depuration fit. Loss parameters—A_0: activity (%; mean ± SD) lost according to the exponential component for dissolved Hg; AE: assimilation efficiency (%; mean ± SD) for trophic Hg; k_e: depuration rate constant (d^{-1}); $Tb_{1/2}$: biological half-life (d; mean ± SD). * = statistically significant difference from other prey and pH conditions of trophic route ($p<0.05$).

Conditions				Uptake			Loss			
Phase	Contamination	pH	Prey	CF_{ss}	k_u	R^2	A_0 or AE	k_e	$Tb_{1/2}$	R^2
Uptake	Dissolved iHg	8.08		709 ± 54	0.136	0.872				
		7.54		893 ± 117	0.097	0.863				
Loss	Dissolved iHg	8.08					96 ± 2	0.016	44 ± 12	0.343
		7.54					105 ± 3	0.013	55 ± 16	0.195
	Trophic MeHg	8.08	Sand goby				98 ± 2	0.002	∞	0.015
		7.54	Sand goby				100 ± 2	0.004	∞	0.054
		8.08	Ditch shrimp				104 ± 2	0.028	25 ± 14*	0.510

Table 2: Distribution of $i^{203}Hg$ (%; mean ± SD) in the tissues of the common cuttlefish, *Sepia officinalis* over time at pH 8.08 and 7.54 during and after dissolved $i^{203}Hg$ exposure. G = gills, BH = branchial hearts, DG = digestive gland, DT = digestive tract, M = mantle muscle, TA = tentacles and arms, BE = beak, OL = optic lobes and R = remaining tissues.

		Uptake 7 d			Uptake 14 d			Loss 21 d		
Conditions	Tissues	Distribution (% ; mean ± SD)			Distribution (% ; mean ± SD)			Distribution (% ; mean ± SD)		
pH 8.08	G	54.5	±	5.6	43.9	±	3.4	43.4	±	9.9
	BH	0.7	±	0.4	2.7	±	3.5	3.0	±	1.3
	DG	11.9	±	1.1	14.5	±	3.4	20.7	±	5.2
	DT	2.9	±	0.7	9.9	±	1.2	6.4	±	2.1
	M	6.9	±	1.7	7.8	±	1.2	6.0	±	3.4
	TA	3.6	±	0.5	3.5	±	0.5	3.3	±	1.0
	BE	0.1	±	0.0	0.1	±	0.0	0.3	±	0.1
	OL	0.8	±	0.2	1.6	±	0.5	1.4	±	0.3
	R	18.9	±	3.2	16.0	±	2.9	15.5	±	3.6
pH 7.54	G	57.7	±	8.5	46.3	±	2.2	50.1	±	5.2
	BH	0.3	±	0.2	0.9	±	0.7	1.6	±	1.0
	DG	8.2	±	3.3	14.3	±	2.6	17.8	±	4.3
	DT	2.4	±	1.8	7.8	±	4.1	6.7	±	2.4
	M	9.6	±	3.0	6.8	±	0.4	6.8	±	0.6
	TA	3.0	±	0.5	3.7	±	0.6	3.2	±	1.0
	BE	0.2	±	0.1	0.1	±	0.0	0.2	±	0.0
	OL	0.9	±	0.4	1.5	±	0.4	1.1	±	0.2
	R	17.8	±	2.6	18.6	±	2.9	12.6	±	2.0

Table 3: Distribution of ^{203}Hg (%; mean ± SD) in the tissues of the common cuttlefish *Sepia officinalis* reared at pH 8.08 and 7.54 and at 4 d and 21 d of depuration following a pulse chase feeding with radiolabelled $Me^{203}Hg$ fish (sand goby) and shrimp (ditch shrimp). G = gills, BH = branchial hearts, DG = digestive gland, DT = digestive tract, M = mantle muscle, TA = tentacles and arms, BE = beak, OL = optic lobes and R = remaining tissues.

		Depuration 4 d			Depuration 21 d		
Condition	Tissues	Radiotracer distribution (% ; mean ± SD)			Radiotracer distribution (% ; mean ± SD)		
Sand goby pH 8.08	G	5.2	±	0.2	3.3	±	0.7
	BH	0.7	±	0.2	0.5	±	0.2
	DG	34.2	±	9.5	8.1	±	1.8
	DT	32.1	±	8.7	21.5	±	5.0
	M	10.2	±	1.2	30.8	±	3.7
	TA	2.3	±	0.3	8.1	±	1.6
	BE	0.3	±	0.1	0.3	±	0.1
	OL	2.3	±	0.4	2.1	±	0.6
	R	12.7	±	2.5	25.3	±	1.6
Sand goby pH 7.54	G	4.2	±	1.1	3.3	±	0.4
	BH	0.6	±	0.3	0.6	±	0.1
	DG	40.8	±	3.7	7.5	±	1.8
	DT	30.7	±	8.4	20.5	±	3.3
	M	7.7	±	2.2	30.8	±	4.0
	TA	2.2	±	0.8	9.4	±	1.0
	BE	0.3	±	0.1	0.3	±	0.1
	OL	2.3	±	0.9	2.3	±	0.4
	R	11.2	±	3.8	25.1	±	3.4
Ditch shrimp pH 8.08	G	2.6	±	1.4	2.6	±	0.5
	BH	0.8	±	0.7	0.6	±	0.2
	DG	71.9	±	12.4	33.8	±	9.8
	DT	6.4	±	3.4	11.5	±	3.5
	M	6.5	±	3.4	22.2	±	2.8
	TA	1.7	±	0.8	6.0	±	2.0
	BE	0.2	±	0.0	0.6	±	0.5
	OL	1.4	±	1.0	1.5	±	0.5
	R	8.6	±	2.5	21.2	±	4.9